

# Inversion of the Oxiranyl Radical Occurs by Quantum-Mechanical Tunneling<sup>1</sup>

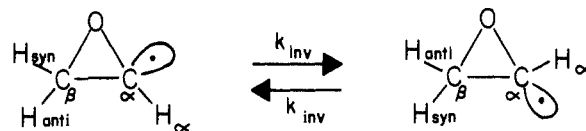
S. Deycard,<sup>2</sup> J. Luszyk, K. U. Ingold,\* F. Zerbetto,<sup>3</sup> M. Z. Zgierski, and W. Siebrand

Contribution from the Division of Chemistry, National Research Council of Canada, Ottawa, Ontario, Canada K1A 0R6. Received February 25, 1988

**Abstract:** Dynamic EPR spectroscopy has been employed to investigate the inversion of the oxiranyl and [2-<sup>2</sup>H]oxiran-2-yl radicals. For the deuterium-substituted radical the inversion can be "frozen" at low temperature, so that the two  $\beta$ -hydrogen atoms can be distinguished ( $a^{\text{H}\beta} = 5.23$  and 4.74 G at 120 K). For the oxiranyl radical the two  $\beta$ -hydrogens do not become distinguishable, but there is some broadening of the central line of the CH<sub>2</sub> triplets at low temperatures. On the basis of the observed difference in  $a^{\text{H}\beta}$  values, the spectra can be simulated, and the simulation can be used to derive temperature-dependent inversion rate constants for the two isotopomers. The results show a large primary isotope effect (factor 5-40, dependent on the temperature) and a curved Arrhenius plot for oxiranyl leading to an invariant low-temperature rate constant for  $T \leq 140$  K. It is therefore concluded that the inversion proceeds by quantum-mechanical tunneling. To investigate this transition quantitatively, an ab initio UHF-MO calculation has been carried out, yielding the molecular geometry, the normal-mode frequencies, and the inversion barrier height. The angle between the C <sub>$\alpha$</sub> -H <sub>$\alpha$</sub>  bond and the plane of the ring is calculated to be much larger than in cyclopropyl (56.5 vs 39.3°) in agreement with the larger  $a^{13\text{C}\alpha}$  (121 G for oxiranyl vs 95.9 G for cyclopropyl) and with the slower inversion. The observed rate constants can be fitted accurately to a modified quartic double-minimum potential, which compares favorably with the effective one-dimensional inversion potential deduced from the quantum-chemical results. The barrier height is estimated to be 6.8 kcal/mol.

Over the past 30 years enormous progress has been made in the measurement of the absolute rate constants and Arrhenius parameters for almost all classes of free-radical reactions in solution. The one class that has been largely neglected is the inversion of nonplanar trivalent radicals.<sup>4</sup> We began our more recent work in this area<sup>5</sup> with a study of the inversion of cyclopropyl and 1-substituted cyclopropyl radicals.<sup>13,14</sup> The rate constants for inversion of the cyclopropyl and 1-methylcyclopropyl radicals were measured at 344 K by a chemical-trapping procedure.<sup>13</sup> We were unable to "freeze" the inversion of the cyclopropyl radical on the EPR time scale even by working at very low temperatures.<sup>13</sup> However, the inversion of 1-methylcyclopropyl could be frozen, and a dynamic EPR study yielded an inversion barrier of 3.1 kcal/mol for this radical.<sup>14</sup> Our results showed that the inversion of cyclopropyl was very much faster than that of 1-methylcyclopropyl, particularly at low temperatures, and we concluded that this was because quantum-mechanical tunneling played a major role in the cyclopropyl inversion.<sup>13-15</sup> However, despite some effort,<sup>16</sup> we have not yet been able to prove that

tunneling is responsible for the rapid inversion of the cyclopropyl radical. We therefore decided to extend our studies to the oxiranyl radical.



It is well established via EPR spectroscopy,<sup>18-21</sup> chemical trapping,<sup>22</sup> and theoretical investigations<sup>18,21,23-27</sup> that the oxiranyl radical and alkylated oxiranyl radicals have a pyramidal configuration at the radical center; i.e., the hydrogen atom, H <sub>$\alpha$</sub> , or alkyl group, R <sub>$\alpha$</sub> , attached to the radical center does not lie in the plane of the three-membered ring. For the oxiranyl radical<sup>21</sup> and for some alkylated oxiranyl radicals,<sup>21,22</sup> there is also evidence for inversion at the radical center. Comparison of these data with those for the inversion of structurally related cyclopropyl radicals indicates that the oxiranyl radicals invert more slowly than the cyclopropyls. For example, Itzel and Fischer<sup>21</sup> obtained a barrier of 5.8 kcal/mol for the inversion of the 2,3-dimethyloxiranyl radical, which is significantly higher than the 3.1 kcal/mol barrier that we found for inversion of the 1-methylcyclopropyl radical.<sup>14,28</sup> For the oxiranyl radical itself, Itzel and Fischer<sup>21</sup> reported that although inversion is too rapid to yield precise kinetic data by EPR spectroscopy, there is a line-broadening effect from which they estimated an inversion barrier of  $2 \pm 1$  kcal/mol. However, this

(1) Issued as NRCC No. 29373.

(2) Canada-France Postdoctoral Exchange Fellow.

(3) NRCC Research Associate.

(4) For a comprehensive survey of absolute kinetic data for organic radicals in solution, see: "Radical Reaction Rates in Liquids". *Landolt-Börnstein, New Series*; Fischer, H., Ed.; Springer-Verlag: Berlin, 1984; Vol. 13, Parts a-e. Kinetic measurements on radical inversions constitute only about 0.1% of the total quantity of kinetic data contained in these five volumes.

(5) Our long-standing interest in radical inversions is attested to by earlier studies on carbon-centered<sup>6-8</sup> and heteroatom-centered<sup>9-12</sup> radicals.

(6) Griller, D.; Ingold, K. U.; Krusic, P. J.; Fischer, H. *J. Am. Chem. Soc.* **1978**, *100*, 6750-6752.

(7) Malatesta, V.; McKelvey, R. D.; Babcock, B. W.; Ingold, K. U. *J. Org. Chem.* **1979**, *44*, 1872-1873.

(8) Griller, D.; Ingold, K. U.; Krusic, P. J.; Smart, B. E.; Wonchoba, E. *R. J. Phys. Chem.* **1982**, *86*, 1376-1377.

(9) Ingold, K. U.; Brownstein, S. *J. Am. Chem. Soc.* **1975**, *97*, 1817-1818.

(10) Compton, D. A. C.; Chatgillaloglu, C.; Mantsch, H. H.; Ingold, K. U. *J. Phys. Chem.* **1981**, *85*, 3093-3100.

(11) Chatgillaloglu, C.; Ingold, K. U.; Scaiano, J. C. *J. Am. Chem. Soc.* **1982**, *104*, 5123-5127.

(12) Ingold, K. U.; Luszyk, J.; Scaiano, J. C. *J. Am. Chem. Soc.* **1984**, *106*, 343-348.

(13) Johnston, L. J.; Ingold, K. U. *J. Am. Chem. Soc.* **1986**, *108*, 2343-2348.

(14) Deycard, S.; Hughes, L.; Luszyk, J.; Ingold, K. U. *J. Am. Chem. Soc.* **1987**, *109*, 4954-4960.

(15) As was first suggested nearly 20 years ago, see: Dewar, M. J. S.; Harris, J. M. *J. Am. Chem. Soc.* **1969**, *91*, 3652-3653.

(16) It has also proved impossible to "freeze" the inversion of  $\alpha$ -deuterio-cyclopropyl on the EPR time scale at temperatures as low as -184 °C in C<sub>2</sub>H<sub>6</sub> as solvent.<sup>17</sup>

(17) Deycard, S., unpublished results.

(18) Dobbs, A. J.; Gilbert, B. C.; Norman, R. O. C. *J. Chem. Soc. A* **1971**, 124-135.

(19) Beckwith, A. L. J.; Tindall, P. K. *Aust. J. Chem.* **1971**, *24*, 2099-2116.

(20) Behrens, G.; Schulte-Frohlinde, D. *Angew. Chem., Int. Ed. Engl.* **1973**, *12*, 932-933.

(21) Itzel, H.; Fischer, H. *Helv. Chim. Acta* **1976**, *59*, 880-901.

(22) Altman, L. J.; Baldwin, R. C. *Tetrahedron Lett.* **1972**, 981-984.

(23) Altman, L. J.; Baldwin, R. C. *Tetrahedron Lett.* **1971**, 2531-2534.

(24) Dobbs, A. J.; Gilbert, B. C.; Norman, R. O. C. *J. Chem. Soc., Perkin Trans. 2* **1972**, 786-794.

(25) Naimushin, A. I.; Zlotskii, S. S.; Zorin, V. V.; Rakhmankulov, D. L. *Vopr. Stereokhim.* **1978**, *7*, 15-20.

(26) Naimushin, A. I.; Zorin, V. V.; Zlotskii, S. S.; Karakhanov, R. A.; Rakhmankulov, D. L. *Dokl. Phys. Chem. (Engl. Transl.)* **1979**, *248*, 800-802.

(27) Naimushin, A. I.; Chuvytkin, N. D.; Lebedev, V. L.; Zlotskii, S. S.; Rakhmankulov, D. L. *Dopov. Akad. Nauk. Ukr. RSR, Ser. B: Geol., Khim. Biol. Nauki*, **1981**, 42-45; *Chem. Abstr.* **1981**, *95*, 114391v.

(28) The 2-methyloxiran-2-yl radical would make a more appropriate comparison. However, in this radical the two  $\beta$ -H's appear to have "accidentally" equivalent hyperfine splittings at temperatures (165 K,<sup>21</sup> 113 K<sup>17</sup>) at which other evidence suggests a frozen configuration on the EPR time scale.<sup>17,21</sup>

**Table I.** Hyperfine Splittings and Their Temperature Dependence for Oxiranyl Radicals in Freon Solvents

radical	T, K	$a^{\text{H}\alpha(\text{D}\alpha)}$ , G	$\frac{\partial a^\alpha}{\partial T}$ , 10 <sup>3</sup> G/deg (T range, K)	$a^{\text{H}\beta(\text{D}\beta)}$ , G	$\frac{\partial a^\beta}{\partial T}$ , 10 <sup>3</sup> G/deg (T range, K)	$a^{13\text{C}\alpha}$ , G	$\frac{\partial a^{13\text{C}\alpha}}{\partial T}$ , 10 <sup>3</sup> G/deg (T range, K)	$a^{13\text{C}\beta}$ , G
	115	24.5		5.06 (2 H)	-3.0 (105-203)			
	124	24.4	4.0 (124-229)	5.3 (2 H)		121.0	21.0 (124-229)	3.0
	120	3.75	0.7 (111-164)	5.23 (1 H) 4.74 (1 H)	-4.2 (111-164) -3.6 (111-164)			
	120	24.4		0.75 (2 D)				

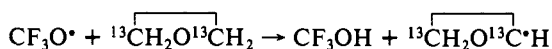
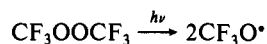
estimate is questionable, and their conclusion that "tunneling is not effectively contributing to the inversion"<sup>21</sup> appears to be unwarranted. On physical grounds a barrier height similar to that of 2,3-dimethyloxiranyl, i.e., ~5.8 kcal/mol, is expected. The value of 2 kcal/mol, obtained from measurements in a narrow temperature range, might be an artifact caused by a curved Arrhenius plot, such curved plots being a characteristic property of tunneling reactions.<sup>29</sup> This interpretation is supported by elementary estimates of the tunneling rate, based on the expected structure and force field of the radical, and would also be implied by our earlier conclusions<sup>13,14</sup> regarding the importance of tunneling in the cyclopropyl inversion.

In general, processes governed by tunneling show a large primary isotope effect as well as a curved Arrhenius plot.<sup>29</sup> To obtain conclusive evidence for tunneling, we have therefore studied the inversion in deuterated oxiranyl. In addition, we have measured the temperature dependence of the inversion rate constants of both normal and deuterium-substituted oxiranyl over the entire range of temperatures where this rate constant can be derived by the present EPR technique. The observed inversion rate constants are fitted to a one-dimensional double-minimum potential, which allows comparison with parameters derived from an ab initio quantum-chemical calculation.

## Results

To study the structure and the inversion kinetics of oxiranyl, we carried out EPR measurements on oxiranyl itself and two isotopomers, namely [2,3-<sup>13</sup>C<sub>2</sub>]oxiranyl, which allowed us to measure the C<sub>α</sub> and C<sub>β</sub> hyperfine splitting (hfs), and α-deuteriooxiranyl ([2-D]oxiran-2-yl), which allowed us to observe the frozen inversion center. These observations in turn allowed us to analyze the kinetics of oxiranyl itself. For this reason, we first present the results of the isotopomers and then those of their parent radical.

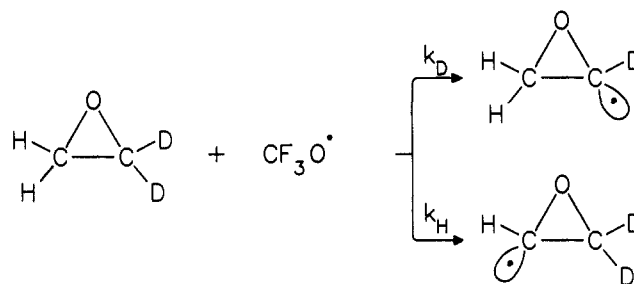
**[2,3-<sup>13</sup>C<sub>2</sub>]Oxiranyl.** The nonplanarity of the radical center in oxiranyl has been deduced from the large absolute value of the hfs of the α-hydrogen and small value of the hfs of the β-hydrogens.<sup>18,19</sup> Since a more direct proof of the oxiranyl radical's nonplanarity would be provided by its C<sub>α</sub> hfs, we first generated [2,3-<sup>13</sup>C<sub>2</sub>]oxiranyl by hydrogen atom abstraction from the parent oxirane with photochemically generated trifluoromethoxy radicals in Freon 12 as solvent at temperatures from 124 to 229 K. Comparison with the EPR spectrum of the unlabeled oxiranyl radical revealed two additional doublet splittings at 124 K: 3.0 G, assigned to C<sub>β</sub>; 121.0 G, assigned to C<sub>α</sub>. The hfs's found in this work for oxiranyl and for isotopically substituted oxiranyls are summarized in Table I.



The large magnitude of the <sup>13</sup>C<sub>α</sub> hfs, viz., 121 G (see Table I), confirms earlier conclusions<sup>18-27</sup> that the radical center in oxiranyls is distinctly pyramidal. Unfortunately, for radicals which contain one or more oxygen atoms directly bonded to the radical center, it is not possible to utilize the magnitude of  $a^{13\text{C}\alpha}$  to calculate the extent to which the radical center has been distorted from planarity.<sup>18,24,30</sup> This is because the extent of loss of spin density at C<sub>α</sub> produced by conjugative electron delocalization to the neighboring oxygen is unknown and, moreover, this positive spin on the oxygen will induce negative spin density at C<sub>α</sub> by spin polarization, which will further decrease the magnitude of the observed C<sub>α</sub> hfs. Qualitatively, it is clear that the out-of-plane angle of the C<sub>α</sub>-H<sub>α</sub> bond in oxiranyl must be greater than in cyclopropyl since the former radical has a significantly larger <sup>13</sup>C<sub>α</sub> hfs (121 G) than the latter (95.9 G)<sup>13</sup> despite the expected spin delocalization onto the neighboring oxygen atom.

The <sup>13</sup>C<sub>β</sub> hfs (3.0 G, see Table I) is considerably smaller than the <sup>13</sup>C<sub>β</sub> hfs in the ethyl radical (13.6 G)<sup>31</sup> and in a number of β-substituted ethyl radicals (10.4-13.7 G),<sup>32</sup> just as would be expected for a nonplanar radical. However, in contrast to the oxiranyl's H<sub>α</sub> hfs, INDO calculations indicate that this <sup>13</sup>C<sub>β</sub> hfs (like that in the planar ethyl radical) has a negative sign (-4.7 G).<sup>18</sup>

**[2-D]Oxiran-2-yl.** The rate of hydrogen tunneling in a chemical or physical process is always dramatically reduced by replacement of the relevant hydrogen by deuterium. We chose [2,2-D<sub>2</sub>]oxirane to produce the title radical together with the [3,3-D<sub>2</sub>]oxiran-2-yl radical at temperatures from 111 to 223 K in Freon 11 or Freon 13 as solvent using photochemically generated CF<sub>3</sub>O<sup>•</sup> radicals:



The relative concentrations of these two radicals can be assumed to be proportional to the relative rates of their formation, i.e., to the relative rate constants for H and D abstraction. At 141 K,  $k_{\text{H}}/k_{\text{D}}$  was found to be 2.9, and a plot of  $\log(k_{\text{H}}/k_{\text{D}})$  vs  $1/T$  ( $121 \text{ K} \leq T \leq 223 \text{ K}$ ) yielded an activation energy difference  $E_{\text{D}} - E_{\text{H}} \approx 0.2 \text{ kcal/mol}$ .

As would be expected from the behavior of the parent oxiranyl radical, the [3,3-D<sub>2</sub>]oxiran-2-yl EPR spectrum showed no significant changes with temperature. However, the EPR spectrum of [2-D]oxiran-2-yl showed dramatic temperature effects. At 141

(29) Bell, R. P. *The Tunnel Effect in Chemistry*; Chapman and Hall: London, 1980.

(30) Brunton, G.; Ingold, K. U.; Roberts, B. P.; Beckwith, A. L. J.; Krusic, P. J. *J. Am. Chem. Soc.* **1977**, *99*, 3177-3179.

(31) Fessenden, R. W. *J. Phys. Chem.* **1967**, *71*, 74-83.

(32) Sciaiano, J. C.; Ingold, K. U.; *J. Phys. Chem.* **1976**, *80*, 275-278.

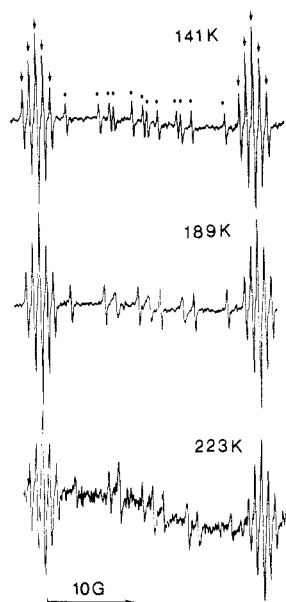


**Figure 1.** EPR spectra obtained from [2,2-D<sub>2</sub>]oxirane during photolysis in the presence of CF<sub>3</sub>OOCF<sub>3</sub> in Freon 11 at different temperatures. The arrows refer to lines assigned to [3,3-D<sub>2</sub>]oxiran-2-yl and the dots to lines assigned to [2-D]oxiran-2-yl.

**Table II.** Rate Constants for Inversion of [2-<sup>2</sup>H]Oxiran-2-yl and Oxiranyl

[2- <sup>2</sup> H]oxiran-2-yl		oxiranyl	
<i>T</i> , K	<i>k</i> <sub>inv</sub> <sup>D</sup> , s <sup>-1</sup>	<i>T</i> , K	<i>k</i> <sub>inv</sub> <sup>H</sup> , s <sup>-1</sup>
141	2.0 × 10 <sup>5</sup>	105	7.0 × 10 <sup>6</sup>
152	5.0 × 10 <sup>5</sup>	109	6.5 × 10 <sup>6</sup>
158	8.0 × 10 <sup>5</sup>	119	6.5 × 10 <sup>6</sup>
166	1.2 × 10 <sup>6</sup>	123	7.0 × 10 <sup>6</sup>
174	2.0 × 10 <sup>6</sup>	135	7.7 × 10 <sup>6</sup>
182	4.0 × 10 <sup>6</sup>	143	8.2 × 10 <sup>6</sup>
188	5.5 × 10 <sup>6</sup>	151	1.2 × 10 <sup>7</sup>
196	7.0 × 10 <sup>6</sup>	161	1.5 × 10 <sup>7</sup>
205	1.0 × 10 <sup>7</sup>	169	2.0 × 10 <sup>7</sup>
223	2.0 × 10 <sup>7</sup>	177	2.5 × 10 <sup>7</sup>
		188	3.5 × 10 <sup>7</sup>
		196	4.5 × 10 <sup>7</sup>
		203	5.5 × 10 <sup>7</sup>

K this radical has a spectrum containing 12 lines of equal intensity (Figure 1), which indicates that at this temperature the inversion of the radical center has been frozen and that the two β-hydrogen atoms are magnetically nonequivalent. At 189 K (Figure 1) the inversion has become rapid enough to cause considerable line broadening, and at 223 K a new pattern of nine lines (triplet of triplets) appears, which indicates that inversion has become rapid on the EPR time scale.

It is not easy to assign the two β-hydrogen hfs's observed in the frozen α-deuteriooxiranyl spectrum. INDO calculations<sup>18,21,33</sup> yield results that are of no diagnostic value. Indeed, Itzel and Fischer<sup>21,33</sup> virtually ignored their own INDO calculations when analyzing the frozen EPR spectra of 2-*tert*-butyloxiran-2-yl (*a*<sub>H<sub>β</sub>(syn)</sub> = 4.8 G, *a*<sub>H<sub>β</sub>(anti)</sub> = 4.6 G, where syn and anti refer to the orbital of the unpaired electron) and of *cis*- and *trans*-2,3-dimethyloxiranyl (*cis*, *a*<sub>H<sub>β</sub>(syn)</sub> = 5.3 G; *trans*, *a*<sub>H<sub>β</sub>(anti)</sub> = 3.8 G), the latter assignments being based on a comparison of the 2-CH<sub>3</sub> hfs of these two isomeric radicals (*cis*, 15.5 G; *trans*, 15.0 G) with the value found for trimethyloxiranyl (15.5 G), in which the 2-CH<sub>3</sub> group must be *cis* to a 3-CH<sub>3</sub> group. We believe Itzel and Fischer's arguments provide a more reliable basis for assignment than the available calculations, and we therefore assign the larger H<sub>β</sub> hfs of α-deuteriooxiranyl to H<sub>β</sub>(syn).

Rate constants for the inversion of this radical, *k*<sub>inv</sub><sup>D</sup> (see Table II), were obtained by matching the experimental EPR spectra

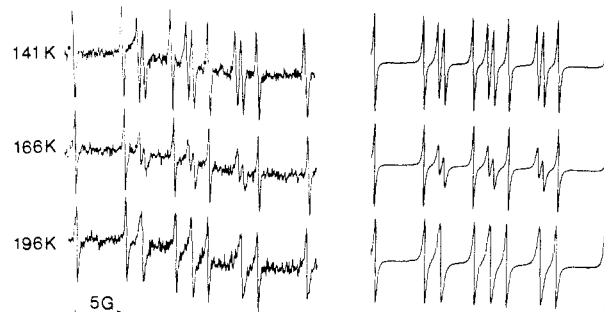


**Figure 2.** Experimental EPR spectra (left) and simulations (right) for α-deuteriooxiranyl at different temperatures. Values of *k*<sub>inv</sub><sup>D</sup> used in the simulations were 2.0 × 10<sup>5</sup> s<sup>-1</sup> (top), 1.2 × 10<sup>6</sup> s<sup>-1</sup> (middle), and 7.0 × 10<sup>6</sup> s<sup>-1</sup> (bottom).

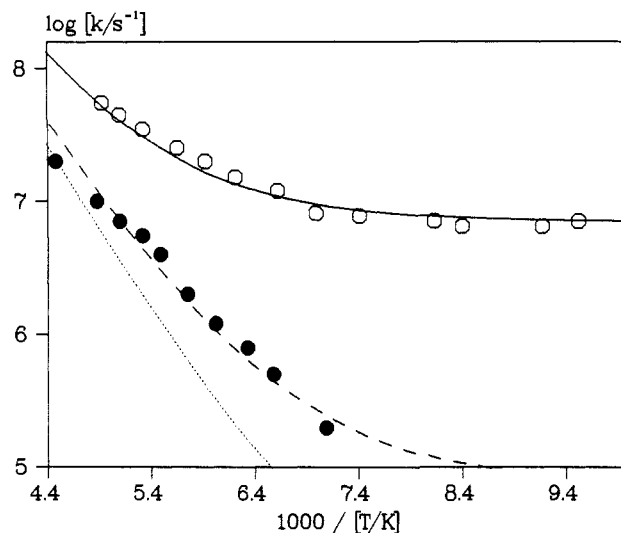


**Figure 3.** Arrhenius plots for the inversion of oxiranyl (○) and α-deuteriooxiranyl (●) radicals. The probable errors in the log *k* (s<sup>-1</sup>) values obtained from Table II are ca. ±0.1 log unit except for α-deuteriooxiranyl at *T* ≤ 150 K and *T* ≥ 200 K, where they are ca. ±0.2 log unit. Solid, dashed, and dotted lines depict calculated rate constants of hydrogen, deuterium, and tritium tunneling, respectively, for the empirical potential displayed in Figure 5.

recorded at various temperatures in the range 141–223 K with spectra simulated in the usual way<sup>34</sup> with different rates for the exchange process (see Figure 2). To maximize the accuracy,<sup>8</sup> the hfs's were obtained by the procedure of Griller and Preston,<sup>35</sup> viz., by measuring the magnetic field and the microwave frequency at the center of each of the 12 lines in the spectrum at temperatures from 111 to 164 K. The temperature coefficients for the two β-hydrogen hfs's that were derived from these measurements are  $-4.2 \times 10^{-3}$  and  $-3.6 \times 10^{-3}$  G/K (see Table I). These two values are equal within our experimental error. We were therefore able to use the mean value found for the difference in the hfs's of the two β-hydrogens in the 111–164 K temperature range in the simulation of all the spectra obtained at higher temperatures where the exchange process becomes observable. This mean difference *a*<sub>H<sub>β</sub>(syn)</sub> – *a*<sub>H<sub>β</sub>(anti)</sub> equals 0.48 G. The line width is, however, temperature dependent for reasons unrelated to the exchange process (as has been found for other alkoxyalkyl radicals)<sup>36</sup> and had to be adjusted for each simulation. The rate constants obtained by these procedures are displayed in Figure 3; they can be fitted to an Arrhenius equation of the form given in eq 1 where  $\theta = 2.3RT$  kcal/mol and the errors represent two standard deviations.

$$\log (k_{\text{inv}}^{\text{D}}/\text{s}^{-1}) = (10.9 \pm 0.2) - (3.6 \pm 0.2)/\theta \quad (1)$$

(34) Heinzer, J. *QCPE* 1972, No. 209.

(35) Griller, D.; Preston, K. F. *J. Am. Chem. Soc.* 1979, 101, 1975–1979.

(36) For example, with the CH<sub>3</sub>OCH<sub>2</sub>· radical, see Figure 1 in ref 37.

(37) Hudson, A.; Root, K. D. *J. Tetrahedron* 1969, 25, 5311–5317.

(33) See footnote 1 in ref 21.



Figure 4. Low-field triplet in the EPR spectrum of the oxiranyl radical in Freon 11 at different temperatures.

**Oxiranyl.** Itzel and Fischer<sup>21</sup> carried out a detailed study of the EPR spectrum of this radical at temperatures down to 134 K and observed a line broadening of the center lines of the CH<sub>2</sub> triplets at temperatures below ca. 165 K. They attributed this to the fact that inversion was becoming slow on the EPR time scale and that the  $\beta$ -hydrogens in a noninverting oxiranyl would be nonequivalent. However, the radical was not observed in a frozen configuration.

We generated the oxiranyl radical by hydrogen abstraction from oxirane with CF<sub>3</sub>O<sup>•</sup> (vide supra) in Freon 13 at temperatures from 105 to 203 K. We observed the same line-broadening effect as Itzel and Fischer<sup>21</sup> (see Figure 4). However, we also observed that there is essentially no further line broadening at temperatures below ca. 140 K. This behavior implies that  $k_{inv}$  has reached a limiting, low-temperature value, which, in turn, strongly suggests that quantum-mechanical tunneling dominates the inversion process at these low temperatures.

It can safely be assumed that the difference in the  $\beta$ -hydrogen hfs's,  $a^{H\beta(syn)} - a^{H\beta(anti)}$ , will be the same for this radical as for  $\alpha$ -deuteriooxiranyl, viz., 0.48 G. It is therefore possible to simulate the line-broadening effect observed for the oxiranyl radical at temperatures in the range 105–203 K. The rate constants,  $k_{inv}^H$ , obtained by matching the experimental and simulated spectra are given in Table II and are shown as an Arrhenius plot in Figure 3. This plot shows the curvature typical for tunneling<sup>29</sup> and reaches a limiting value  $k_{inv}^H(T \rightarrow 0) \approx 7 \times 10^6 \text{ s}^{-1}$  for  $T \lesssim 140 \text{ K}$ .

#### Calculations

**Ab Initio MO Treatment.** To interpret these results quantitatively, we need to know the structure and the vibrational force field of oxiranyl. Since no reliable experimental data are available, we carried out an ab initio molecular orbital calculation aimed at providing a reasonably accurate description of the inversion potential. Using the GAMESS program,<sup>38</sup> we optimized the molecular geometry and calculated the normal-mode coordinates and frequencies at the UHF-6-31 G\*\* level<sup>39</sup> of theory for two stationary conformations: the C<sub>1h</sub> conformation with the H <sub>$\alpha$</sub>  atom

Table III. Energies (Hartrees), Relative Energies (cm<sup>-1</sup>), and Zero-Point Energy Corrections  $\sum_k \epsilon_{k0}$  (cm<sup>-1</sup>) with  $k = 1-11$  and Barrier Heights<sup>a</sup> (cm<sup>-1</sup>) for Oxiranyl and  $\alpha$ -Deuteriooxiranyl

conformn	C <sub>1</sub>	C <sub>1h</sub>
<i>E</i>	-152.23379	-152.21949
$\Delta E$	0	3137
$\sum_k \epsilon_{k0}^H$	10008	9981
$\sum_k \epsilon_{k0}^D$	9345	9368
<i>E<sub>b</sub><sup>H</sup></i>		3110
<i>E<sub>b</sub><sup>D</sup></i>		3160

$$^a E_b = \Delta E + \sum_{k=1}^{11} \epsilon_{k0}(C_{1h}) - \sum_{k=1}^{11} \epsilon_{k0}(C_1).$$

Table IV. Bond Lengths (Å) and Out-of-Plane Angles for Oxiranyl

conformn	C <sub>1</sub>	C <sub>1h</sub>
C <sub><math>\alpha</math></sub> C <sub><math>\beta</math></sub>	1.438	1.421
C <sub><math>\alpha</math></sub> O	1.354	1.353
C <sub><math>\beta</math></sub> O	1.427	1.441
C <sub><math>\alpha</math></sub> H <sub><math>\alpha</math></sub>	1.076	1.061
C <sub><math>\beta</math></sub> H <sub><math>\beta</math></sub> <sup>a</sup>	1.078	1.078
C <sub><math>\beta</math></sub> H <sub><math>\beta</math></sub> <sup>a</sup>	1.077	1.078
$\angle C_{\alpha}H_{\alpha}$	56.52°	0
$\angle H_{\beta}C_{\beta}H_{\beta}$ <sup>a</sup>	115.55°	115.10°

<sup>a</sup>H <sub>$\beta$</sub>  is anti and H <sub>$\beta'$</sub>  is syn relative to the orbital of the unpaired electron.

Table V. Calculated Normal-Mode Frequencies (cm<sup>-1</sup>) and Displacements [C<sub>1</sub> Relative to C<sub>1h</sub> in Å·amu<sup>1/2</sup>] of Oxiranyl

<i>k</i>	assignt <sup>a</sup>	$\omega_k(C_1)^b$	$\omega_k(C_{1h})^b$	sym (C <sub>1h</sub> )	$\Delta_k$
1	asym C <sub><math>\beta</math></sub> H <sub><math>\beta</math></sub> stretching	3368	3351	a''	0.032
2	C <sub><math>\alpha</math></sub> H <sub><math>\alpha</math></sub> stretching	3337	3525	a'	-0.242
3	sym C <sub><math>\beta</math></sub> H <sub><math>\beta</math></sub> stretching	3276	3266	a'	-0.031
4	CH <sub>2</sub> deformation	1669	1671	a'	0.024
5	ring stretching	1471	1475	a'	-0.075
6	CH wagging	1323	1338	a'	-0.060
7	sym CH bending	1249	1193	a'	-0.034
8	asym CH bending	1185	1064/999 <i>i</i>	a''	0.375
9	CH <sub>2</sub> twisting	1171	1189	a''	0.126
10	ring deformation	1035	1024	a'	-0.164
11	ring deformation	932	866	a'	0.212
12	C <sub><math>\alpha</math></sub> H <sub><math>\alpha</math></sub> bending	883	1064/999 <i>i</i>	a''	0.491

<sup>a</sup>The assignment refers to the principal component of the normal coordinates. Many modes are thoroughly mixed. <sup>b</sup>The method used tends to yield frequencies that are too high by up to 10%.<sup>48</sup>

Table VI. Calculated Normal-Mode Frequencies (cm<sup>-1</sup>) and Displacements [C<sub>1</sub> Relative to C<sub>1h</sub> in Å·amu<sup>1/2</sup>] of  $\alpha$ -Deuteriooxiranyl

<i>k</i> <sup>a</sup>	assignt <sup>b</sup>	$\omega_k(C_1)^c$	$\omega_k(C_{1h})^c$	sym (C <sub>1h</sub> )	$\Delta_k$
1	asym C <sub><math>\beta</math></sub> H <sub><math>\beta</math></sub> stretching	3367	3351	a''	-0.001
2	C <sub><math>\alpha</math></sub> D <sub><math>\alpha</math></sub> stretching	2468	2628	a'	-0.332
3	sym C <sub><math>\beta</math></sub> H <sub><math>\beta</math></sub> stretching	3278	3266	a'	0.006
4	CH <sub>2</sub> deformation	1665	1666	a'	0.047
5	ring stretching	1452	1433	a'	0.132
6	CH <sub>2</sub> wagging	1312	1329	a'	-0.023
7	CH <sub>2</sub> twisting	1215	1189	a''	0.015
8	CH <sub>2</sub> bending	1122	1058	a''	-0.231
9	ring deformation	1085	1137	a'	0.024
10	sym C <sub><math>\alpha</math></sub> D <sub><math>\alpha</math></sub> bending	853	752	a'	0.361
11	ring deformation	950	925	a'	-0.004
12	asym C <sub><math>\alpha</math></sub> D <sub><math>\alpha</math></sub> bending	707	783 <i>i</i>	a''	0.768

<sup>a</sup>The numbers are chosen so as to yield the closest correspondence to the modes of oxiranyl listed in Table V. The correspondence is modest for modes 7, 8, and 10 and poor for 9 and 11. <sup>b</sup>See Table V, footnote a. <sup>c</sup>See Table V, footnote b.

in the COC plane and the stable C<sub>1</sub> conformation with H <sub>$\alpha$</sub>  out of the plane. The calculated structural parameters and energies are listed in Tables III and IV, respectively. The normal-mode frequencies of both conformations and the corresponding normal-coordinate displacements of the C<sub>1</sub> relative to the C<sub>1h</sub> conformation for oxiranyl and  $\alpha$ -deuteriooxiranyl are listed in Tables V and VI, respectively. In the C<sub>1h</sub> conformation, one of the frequencies is imaginary, since the C <sub>$\alpha$</sub> H <sub>$\alpha$</sub>  out-of-plane bending

(38) Dupuis, M.; Spangler, D.; Wendoloski, J. J. *NRCC Software Catalog*, Program QG01, Lawrence Berkeley Laboratory, Livermore, CA, 1980; Vol. 1. Schmidt, M.; Elbert, S.; Lam, B. *GAMESS User's Guide* (NDSU).

(39) Francl, M. M.; Pietro, W. J.; Hehre, W. J.; Binkley, J. S.; Gordon, M. S.; DeFrees, D. J.; Pople, J. A. *J. Chem. Phys.* **1982**, *77*, 3654–3665. Hariharan, P. C.; Pople, J. A. *Theor. Chim. Acta* **1973**, *28*, 213–222.

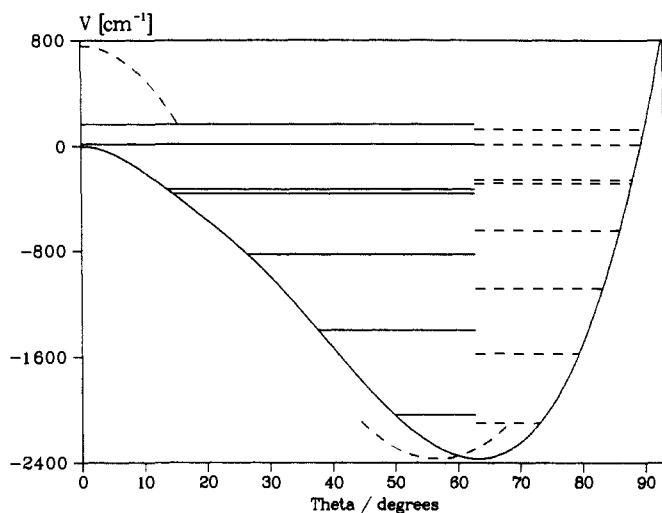


**Figure 5.** Half of the symmetrical double-minimum potential governing the inversion of oxiranyl plotted against the  $C_{\alpha}H_{\alpha}$  out-of-plane angle. The solid curve depicts the empirical potential obtained by fitting the observed rate constants as in Figure 3. The broken curves depict calculated parts of the potential, namely, the position, energy, and curvature of the stationary points, obtained quantum chemically. Horizontal solid and broken lines depict the energy levels associated with the solid-curve potential for oxiranyl and  $\alpha$ -deuteriooxiranyl, respectively.

potential reaches a maximum for this conformation. The normal-coordinate displacements  $\Delta_k$  were calculated from the atomic displacements  $r_i$  by multiplying the vector of the mass-weighted atomic displacements  $m_i^{1/2}r_i$  by the  $3N(3N-6)$  matrix  $L$  describing normal coordinates in terms of mass-weighted Cartesian coordinates of  $C_1$ .<sup>40</sup>

As expected, the  $C_{\alpha}H_{\alpha}$  out-of-plane bending mode  $\nu_{12}$  shows the strongest displacement, but other modes such as the asymmetric CH bending mode  $\nu_8$  and the  $C_{\alpha}H_{\alpha}$  stretching mode  $\nu_2$  are also strongly displaced. The minimum-energy path of  $H_{\alpha}$  during the inversion involves not only components perpendicular to the COC plane but also components parallel to the plane. Moreover, atoms other than  $H_{\alpha}$  also undergo substantial displacement between  $C_1$  and  $C_{1h}$ . Hence, to calculate the inversion rate constant accurately, we would need to consider a multidimensional potential energy surface.

**Tunneling Rate Constants.** For practical reasons, we restrict ourselves here to an approximate calculation of the inversion rate constant based on a one-dimensional effective potential. Since the main contributions to the effective displacement come from CH bending vibrations with roughly the same reduced mass and frequency, this may not be a bad approximation. For the frequency associated with the effective potential, we take the  $C_{\alpha}H_{\alpha}$  out-of-plane frequency  $\omega_{12}$  in the  $C_1$  conformation since it dominates and has the lowest frequency, so that it will contribute most to the temperature dependence at low temperatures. Since the actual minimum-energy path of the inversion is not completely defined by our stationary-points calculation, we take the effective displacement  $\Delta$  to be equal to the norm of the normal-mode displacements<sup>40</sup> (eq 2). The barrier height is obtained from Table

$$\Delta = \left( \sum_k \Delta_k^2 \right)^{1/2} \quad \Delta_k = \sum_i m_i^{1/2} r_i L_{ik} \quad (2)$$

IV, and the curvature at the top of the barrier is determined by  $i\omega_{12}$  in the  $C_{1h}$  conformation. The resulting partial potential is depicted by broken curves in Figure 5, where the effective displacement  $\Delta$  is represented by its angular component  $\theta$  along the  $C_{\alpha}H_{\alpha}$  out-of-plane bending coordinate.

Since this is a partial potential, defined only at stationary points, we cannot use it directly to calculate inversion rate constants. We therefore use a reverse procedure and derive an empirical potential from the observed rate constants. The simplest double-minimum

potential is the quartic potential (eq 3) with an equilibrium dis-

$$V = Aq^4 - Bq^2 \quad (3)$$

tance  $\bar{q} = (B/2A)^{1/2}$ , a barrier height  $E_b = B^2/4A$ , and top ( $q = 0$ ) and bottom ( $q = \bar{q}$ ) curvatures corresponding to  $i\omega(0) = 2^{1/2}B$  and  $\omega(\bar{q}) = 2B$ . Using  $A$  and  $B$  as adjustable parameters, we solve the corresponding Schrödinger equation numerically. The eigenvalues below the top of the barrier are arranged in closely spaced pairs  $\epsilon_v^{\pm}$  where  $|\epsilon_v^+ - \epsilon_v^-|$  is the splitting due to tunneling associated with the  $v$ th vibrational level of the  $C_{\alpha}H_{\alpha}$  out-of-plane vibration. We take the corresponding transition rate constants to be<sup>29,41</sup> that given in eq 4. The inversion rate constant is then given by eq 5 where  $\epsilon_v = 1/2(\epsilon_v^+ + \epsilon_v^-)$ . For levels  $\epsilon_v > E_b$ , we take  $k_v = 10^{13} \text{ s}^{-1}$ .

$$k_v = 2|\epsilon_v^+ - \epsilon_v^-|/h \quad (4)$$

$$k_{\text{inv}}(T) = \sum_v [k_v \exp(-\epsilon_v/k_B T)] / \sum_v \exp(-\epsilon_v/k_B T) \quad (5)$$

We assume that oxiranyl and  $\alpha$ -deuteriooxiranyl have the same barrier  $E_b$ . Strictly speaking, we should correct  $E_b$  for the difference in zero-point energy for modes  $\nu_1 - \nu_{11}$  between  $C_1$  and  $C_{1h}$ , which would lead to slightly different values for the two isotopomers, but this zero-point correction is so small (see Table III) that it can be safely neglected. The parameters  $A$  and  $B$  for oxiranyl and  $\alpha$ -deuteriooxiranyl differ then only by the ratio  $\omega_{12}^D/\omega_{12}^H = 0.80$ , viz.  $A^D = 0.80A^H$  and  $B^D = 0.80B^H$ .

It turns out that we can get a good fit to both the absolute values and the temperature dependence of the observed rate constants  $k_{\text{inv}}^H(T)$  and  $k_{\text{inv}}^D(T)$  for suitably chosen  $A$  and  $B$  values. With  $q$  dimensionless, we have  $A^H = 12.47 \text{ cm}^{-1}$  and  $B^H = 335 \text{ cm}^{-1}$ . The corresponding fit is very similar to that shown in Figure 3 (solid and broken lines for  $k^H$  and  $k^D$ , respectively), but the potential itself does not compare well with the calculated potential. This is due to the fact that the quartic potential leads to a curvature at the bottom that amounts to  $2^{1/2}$  times that at the top whereas this ratio is calculated to be smaller than unity. To correct this, we introduce the modified quartic potential in eq 6, which allows

$$V(q) = (Aq^4 - Bq^2)[1 + \exp(-Cq^2)] \quad (6)$$

for stronger curvature at the top of the barrier without affecting the bottom. The fit displayed in Figure 3 has been obtained with this potential for  $A^H = 12.37 \text{ cm}^{-1}$ ,  $B^H = 343 \text{ cm}^{-1}$ , and  $C = 1$ . The corresponding potential, plotted as a function of the out-of-plane angular component of the tunneling coordinate, is depicted in Figure 5 (solid curve). Comparison with the calculated parts of the potential, depicted by broken lines in Figure 5, indicates that the agreement is satisfactory, although not perfect. The energy levels  $\epsilon_v^{\pm}$  corresponding to the empirical potential are shown as solid lines for oxiranyl and broken lines for  $\alpha$ -deuteriooxiranyl.

## Discussion

No attempt will be made to achieve a quantitative interpretation of the hfs constants and their temperature dependence. The work of Knight et al.,<sup>42</sup> who studied simpler radicals using much more elaborate methods, indicates that it would be unrealistic to expect the present method to yield accurate spin densities. Qualitatively, the observed positive temperature dependence of the  $C_{\alpha}$  and  $H_{\alpha}$  hfs constants can be explained, following Krusic and Meakin,<sup>43</sup> as the result of thermal averaging over the levels of the double-minimum inversion potential.

The observed inversion rate constants  $k_{\text{inv}}^H(T)$  and  $k_{\text{inv}}^D(T)$ , that are listed in Table II and are displayed in Figure 3, show prima facie evidence of quantum-mechanical tunneling, namely (i) a large primary isotope effect and (ii) a curved Arrhenius plot for  $k_{\text{inv}}^H(T)$ . Although the data for  $k_{\text{inv}}^D(T)$  can be fitted to yield a straight Arrhenius plot, the resulting preexponential (frequency)

(41) Miller, W. H. *J. Phys. Chem.* **1979**, *83*, 960-963.

(42) Knight, L. B., Jr.; Johannessen, K. D.; Cobranchi, D. C.; Earl, E. A.; Feller, D.; Davidson, E. R. *J. Chem. Phys.* **1987**, *87*, 885-897. Knight, L. B., Jr.; Ligon, A.; Woodward, R. W.; Feller, D.; Davidson, E. R. *J. Am. Chem. Soc.* **1985**, *107*, 2857-2864.

(43) Krusic, P. J.; Meakin, P. *J. Am. Chem. Soc.* **1976**, *98*, 228-230.

(40) Zerbetto, F.; Zgierski, M. Z.; Orlandi, G. *Chem. Phys. Lett.* **1987**, *139*, 401-406.

**Table VII.** Calculated Normal-Mode Frequencies ( $\text{cm}^{-1}$ ) and Displacements [ $C_1$  Relative to  $C_{1h}$  in  $\text{\AA}\cdot\text{amu}^{1/2}$ ] of  $\alpha$ -Tritiooxiranyl

$k^a$	assign <sup>b</sup>	$\omega_k(C_1)^c$	$\omega_k(C_{1h})^c$	sym ( $C_{1h}$ )	$\Delta_k$
1	asym $C_\beta H_\beta$ stretching	3367	3351	$a''$	-0.001
2	$C_\alpha T_\alpha$ stretching	2119	2277	$a'$	-0.376
3	sym $C_\beta H_\beta$ stretching	3278	3266	$a'$	0.006
4	$\text{CH}_2$ deformation	1661	1662	$a'$	-0.073
5	ring stretching	1429	1387	$a'$	0.201
6	$\text{CH}_2$ wagging	1311	1327	$a'$	-0.026
7	$\text{CH}_2$ twisting	1213	1189	$a''$	-0.017
8	$\text{CH}_2$ bending	1108	1055	$a''$	0.171
9	ring deformation	1075	1129	$a'$	0.054
10	sym $C_\alpha T_\alpha$ bending	751	662	$a'$	0.408
11	ring deformation	936	903	$a'$	0.094
12	asym $C_\alpha T_\alpha$ bending	620	696i	$a''$	0.878

<sup>a</sup>See Table VI, footnote a. <sup>b</sup>See Table V, footnote a. <sup>c</sup>See Table V, footnote b.

factor of  $10^{11} \text{ s}^{-1}$  is too small by 2 orders of magnitude to allow interpretation of the inversion as a classical (over-the-barrier) process. Indeed, the preexponential factors for inversion of 1-methylcyclopropyl<sup>14</sup> and 2,3-dimethyloxiranyl<sup>21</sup> are  $10^{13.1}$  and  $10^{12.6} \text{ s}^{-1}$ , respectively. Hence, the apparent linearity of the Arrhenius plot of  $k_{\text{inv}}^{\text{D}}(T)$  must be an artifact resulting from the narrowness of the temperature range in which these rate constants can be measured.

This is confirmed by the theoretical analysis based on an ab initio evaluation of the structure of the radical and its vibrational potential near the stationary points of the potential energy surface. The resulting partial inversion potential is close enough to the one-dimensional empirical potential derived from the observed inversion rate constants to confirm the validity of this interpretation. In particular, the rate constants  $k_{\text{inv}}^{\text{D}}(T)$  for  $\alpha$ -deuteriooxiranyl smoothly fit a curved Arrhenius plot. Note that the strongest curvature of this plot occurs at lower temperatures than that of the  $k_{\text{inv}}^{\text{H}}(T)$  plot, since the frequency of the out-of-plane bending mode is lower in the deuterio radical, so that its excited states start contributing to the tunneling at lower temperatures. The limiting rate constant  $k_{\text{inv}}^{\text{D}}(0)$  at 0 K is calculated to be  $6.9 \times 10^4 \text{ s}^{-1}$ .

The good agreement between the theoretical and the empirical tunneling potential observed for oxiranyl indicates that, to a first approximation, this inversion can indeed be treated as a one-dimensional process involving a single oscillator. In earlier treatments<sup>44-46</sup> of hydrogen-transfer reactions in which the hydrogen atom is transferred between two different atoms, a two-dimensional treatment was found to be a minimum requirement. In particular, it was concluded that modes affecting the separation of the atoms between which hydrogen is transferred must be included since they govern the temperature dependence of the transfer. In the present case, there are no such modes. Moreover, the vibrations along the reaction coordinate, which govern the transition, are the lowest frequency modes of the radical and hence determine the temperature dependence of the tunneling at low temperatures. Most of them are CH bending modes with comparable frequencies and reduced masses, so that they can be combined into a single "effective" mode. The one exception, namely the  $C_\alpha H_\alpha$  (or  $C_\alpha D_\alpha$ ) stretching mode, has such a high frequency that it cannot contribute significantly to the temperature dependence for the system at hand.

Comparing the empirical and calculated potentials, we note that the empirical  $C_\alpha H_\alpha$  out-of-plane angle of  $63.2^\circ$  is larger than the calculated angle of  $56.5^\circ$ , which we expect to be accurate.<sup>47</sup> The overestimate of this angle lengthens the tunneling path and hence compensates for the absence of components of the inversion mode that are neglected in our one-dimensional approximation. The empirical frequency of  $685 \text{ cm}^{-1}$ , deduced from eq 6 for the bottom of the potential of Figure 5, is smaller than the calculated frequency of  $883 \text{ cm}^{-1}$ , which, however, is expected to be too high by up to 10%.<sup>48</sup> The remaining discrepancy of about 15-20% compensates for the temperature dependence caused by modes excluded from the model. The empirical barrier height of 6.8 kcal/mol is smaller than the calculated height of 8.9 kcal/mol but in excellent agreement with the experimental barrier height for 2,3-dimethyloxiranyl, which amounts to<sup>21</sup> 7.0 kcal/mol after correction for the zero-point energy. Considering the expected accuracy of our calculations, we accept the empirical value for the barrier height as more reliable than the calculated value.

Although the true inversion potential is multidimensional, these numbers confirm that the one-dimensional potential is a reasonably accurate approximation. It is of course much more pictorial than the full potential energy surface and gives, in combination with the calculated structure and force field, a clear and concise picture of the inversion dynamics of the radical.

This potential allows us to estimate the inversion rate constant for the tritium-substituted isotopomer [2-T]oxiran-2-yl. The corresponding normal-mode frequencies in the  $C_1$  and  $C_{1h}$  conformations and the corresponding displacements between these conformations are listed in Table VII. The calculated inversion rate constants are depicted by a dotted line in Figure 3; the limiting value at 0 K is predicted to be  $2 \times 10^3 \text{ s}^{-1}$ . No experimental data are available for this isotopomer.

The present model is easily adapted to other inversion reactions involving hydrogen tunneling. For instance, it allows one to estimate the inversion rate constants for cyclopropyl. On the basis of a theoretical  $C_\alpha H_\alpha$  out-of-plane angle of<sup>49</sup>  $39.3^\circ$ , an experimental barrier height (for methylcyclopropyl) of 3.1 kcal/mol,<sup>14</sup> and the same harmonic out-of-plane frequencies as oxiranyl, we estimate limiting low-temperature values  $k_{\text{inv}}^{\text{H}}(0) = 10^{11} \text{ s}^{-1}$  and  $k_{\text{inv}}^{\text{D}}(0) = 10^{10} \text{ s}^{-1}$  and qualitatively the same temperature dependence as for oxiranyl and  $\alpha$ -deuteriooxiranyl, respectively. These numbers are probably upper limits since a slightly larger empirical angle is expected (as found for oxiranyl), leading to a reduced tunneling rate. The observation<sup>16</sup> that the inversion of  $\alpha$ -deuteriocyclopropyl cannot be frozen on the EPR time scale at low temperatures supports these estimates. The same calculations yield  $k_{\text{inv}}^{\text{H}}(344) \approx 6 \times 10^{11} \text{ s}^{-1}$ , in qualitative agreement with the estimate of ca.  $10^{12} \text{ s}^{-1}$  at 344 K, derived from trapping experiments.<sup>13</sup>

## Experimental Section

**Materials.** Oxirane (Canadian Liquid Air, Ltd.), [2,3-<sup>13</sup>C<sub>2</sub>]oxirane (MSD Isotopes), [2,2-<sup>2</sup>H<sub>2</sub>]oxirane (MSD Isotopes), Freons 11, 12, and 13 (Matheson), and bis(trifluoromethyl) peroxide (PCR Research Chemicals) were used as received.

**EPR Measurements.** Spectra were recorded on a Varian E104 EPR spectrometer. Radicals were generated by UV photolysis using a 1000-W Hg-Xe lamp on deaerated samples containing the oxirane, peroxide, and Freon that had been sealed under vacuum.

Registry No. Oxiranyl radical, 31586-84-2.

(44) Siebrand, W.; Wildman, T. A.; Zgierski, M. Z. *J. Am. Chem. Soc.* **1984**, *106*, 4083-4089.

(45) Siebrand, W.; Wildman, T. A.; Zgierski, M. Z. *J. Am. Chem. Soc.* **1984**, *106*, 4089-4096.

(46) Doba, T.; Ingold, K. U.; Siebrand, W.; Wildman, T. A. *Faraday Discuss. Chem. Soc.* **1984**, *78*, 175-191.

(47) Pulay, P.; Fogarasi, G.; Boggs, J. E. *J. Chem. Phys.* **1981**, *74*, 3999-4014. Pulay, P. In *Applications of Electronic Structure Theory*; Schaefer, H. F., Ed. Plenum: New York, 1977.

(48) Hehre, W. J.; Radom, L.; Schleyer, P. v. R.; Pople, J. A. *Ab Initio Molecular Orbital Theory*; Wiley: New York, 1986.

(49) Dupuis, M.; Pacansky, J. *J. Chem. Phys.* **1982**, *76*, 2511-2515.